CPW Fed Conformal Folded Dipole with Pattern Diversity for 5G Mobile Terminals

Gulur S. Karthikeya, Mahesh P. Abegaonkar*, and Shiban K. Koul

Abstract—A coplanar waveguide (CPW) fed folded dipole with a 20% impedance bandwidth and 4–6 dBi endfire gain with stable patterns is proposed. Since the proposed element is electrically large $(2.1\lambda \times 2\lambda)$ conformal topology of this endfire radiator is designed and characterized. The input impedance is not altered significantly compared to the planar element. The radiation in the H plane indicates an increase in specific absorption rate when integrated with a typical mobile terminal. In order to mitigate this effect, a compact $(0.8\lambda \times 0.8\lambda)$ wideband reflector with periodic sinusoidal slots is proposed and mounted with the conformal element at an offset of 0.2λ from the radiator. The proposed antenna has an operating bandwidth from 24 to 30 GHz (20%) with an endfire gain of 6–7 dBi across the band. The front to back ratio is more than 12 dB across the band. Pattern diversity of the conformal antenna is also investigated. Simulated and measurement results are presented in detail.

1. INTRODUCTION

The exponential growth in data consumption by the smartphone users across the globe has prompted microwave engineers to design, develop and deploy transceiver systems capable of handling high datarates [1]. The existing infrastructure is facing a major crunch with respect to the datarates offered per user. In order to enhance the datarates, mmWave bands have been promoted as the future candidate for 5G cellular telephony according to experts in academia and research organizations [2]. 28 GHz band is one of the hot favorites for the proposed 5G telecommunication hardware ecosystem. The inherent problem associated with frequencies beyond 20 GHz is the high path loss and penetration loss as reported in [3]. The major challenge for the hardware designers is to mitigate this effect with a feasible solution on the mobile terminal and base station for the available link budget for the communication system [4]. The standard approach to solve this problem is to increase the radiating aperture of the antennas on the mobile terminal to compensate for the path loss [5].

The desirable features of antennas integrated on a 5G mobile terminal include conformal structure hence occupying least volume to achieve the desired gain, low specific absorption rate, high impedance bandwidth to facilitate future bands near 28 GHz, and high gain for the available aperture at the mobile front-end. Pattern diversity is also a desired feature to support the landscape and portrait modes of the smartphone [6]. Several designs for antennas to be integrated on 5G mobile terminals have been proposed. For instance the multilayered antenna array would increase the complexity, and the aperture size might be unsuitable for mobile terminals [7]. The circularly polarized narrowband high gain element proposed in [8] has an aperture of 25×25 mm, which exceeds the available space in a mobile terminal. The antenna designed in [9] has 58% wideband with stable patterns and a reasonable gain of 6–8 dBi but suffers from high SAR, if integrated on a mobile terminal. The radiation patterns of the strongly resonant structure reported in [10] are unusable for the mobile terminal in any feasible orientation. It must be noted that most of the reported papers have planar design with microstrip feed.

The fabrication process described in [11] to realize a conformal antenna element could be redesigned for the 28 GHz band, but the dielectric mount supporting the radiating element would create an impedance mismatch in addition to reduction in gain.

The conformal antenna array of [12] has a large electrical footprint and hence might lead to distortions in the beam when scaled to the 28 GHz band. The 60 GHz antenna array of [13] has a conformal radius of 25 mm translating to 2.5λ at 28 GHz indicating a large physical footprint of the element. A uniplanar feed mechanism would be preferred for smooth transition in a conformal architecture. Conformal designs also lack pattern diversity for integration with mobile terminal.

CPW feed for antenna is readily feasible for substrates with relatively higher dielectric constant at lower operating frequencies below X band [14]. The gap width in the CPW line would be plausible with the standard chemical etching method for the aforementioned criteria. Also, uniplanar feeding technique is popular beyond 60 GHz due to the application of micro-fabrication processes and the probe stations utilized for antenna characterizations [15]. The CPW-fed element proposed in [16] has a wideband but low gain 1.5–4 dBi. The triple band antenna in [17] has a narrow bandwidth at 30 GHz, and an airbridge is part of the feedline for impedance match.

Hence, a CPW-fed wideband element with stable patterns and endfire gain has been proposed. Conformal architecture has also been investigated with pattern diversity. The proposed CPW-fed folded dipole element is presented in Section 2 followed by its characterization of its conformal counterpart in Section 3. The wideband reflector design and integration are discussed in Section 4.

2. CPW FED FOLDED DIPOLE

The proposed CPW-fed folded dipole is illustrated in Figure 1(a) and is designed on a Nelco NY9220 substrate with ε_r of 2.2 and 20 mil thickness. A low dielectric constant is selected to reduce additional
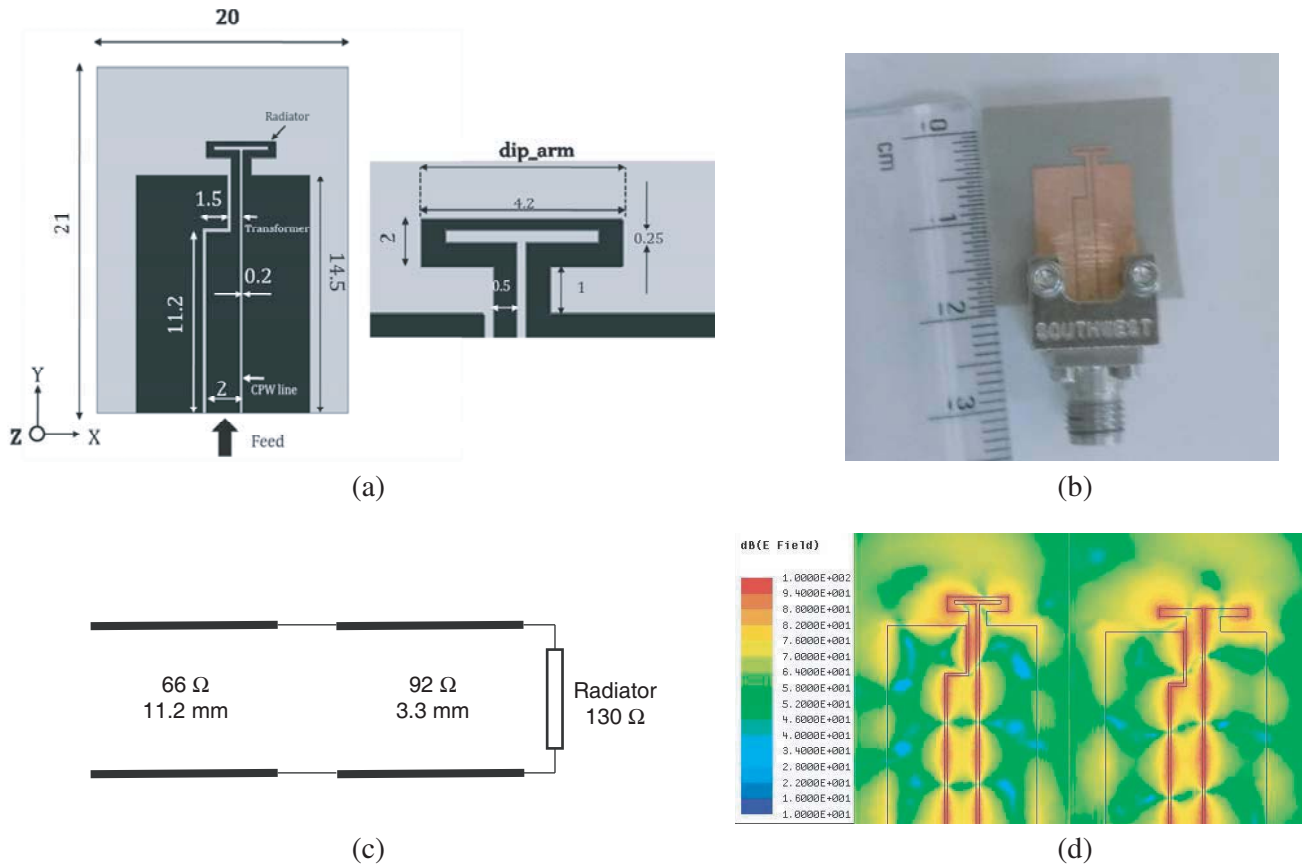
Figure 1. (a) CPW fed folded dipole design. (b) Photograph of the folded dipole. (c) Equivalent circuit of the antenna. (d) E field plots of folded and conventional dipole.

modes of surface waves. An electrically thin substrate, 0.05λ, was chosen to minimize cross-pol radiation in the endfire. The chosen CPW line has a characteristic impedance of $66\,\Omega$ [18] and is connected to a stepped impedance transformer of high impedance of $92\,\Omega$ which acts as a CPW to CPS transition feeding the input impedance of $130\,\Omega$ of the folded dipole. The equivalent circuit is shown in Figure 1(c). This topology was simulated in ADS to verify the characteristics of the input reflection coefficient of the proposed antenna. A conventional half-wave printed dipole with CPW feed and appropriate impedance transformer was also investigated. The E field plots of folded dipole and conventional dipole at $28\,$GHz are illustrated in Figure 1(d). The length of the dipole arms is $2.85\,$mm, and the impedance transformer creates a narrowband transition from the CPW feed line and the radiating arms hence leading to a 10% impedance bandwidth with poor front to back ratio. The radiator is more than 1.5λ away from the feed, and ground width is chosen to ensure proper grounding contact with the end-launch connector with a reasonable pattern in the E plane.

The input reflection coefficient with respect to variation in 'dip_arm' is shown in Figure 2(a). It is observed that when dipole is below $3\,$mm, the antenna has poor impedance match and over $5\,$mm which creates an over-moded antenna for the designed feedline and transformer. Hence, $4.2\,$mm is chosen as the length of the dipole arm, whose $|S_{11}|$ is shown in Figure 2(b). The simulations were performed in Ansys HFSS. The $10\,$dB bandwidth is from 24 to $30\,$GHz. The return loss characteristics are maintained
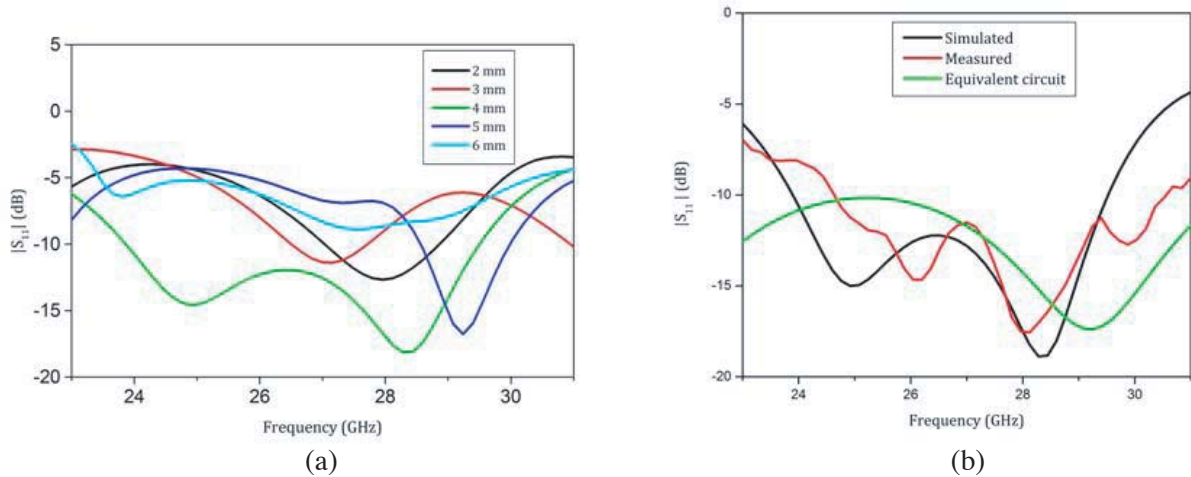
Figure 2. (a) $|S_{11}|$ variation with dip_arm. (b) $|S_{11}|$ of the proposed folded dipole.

(a)

(b)
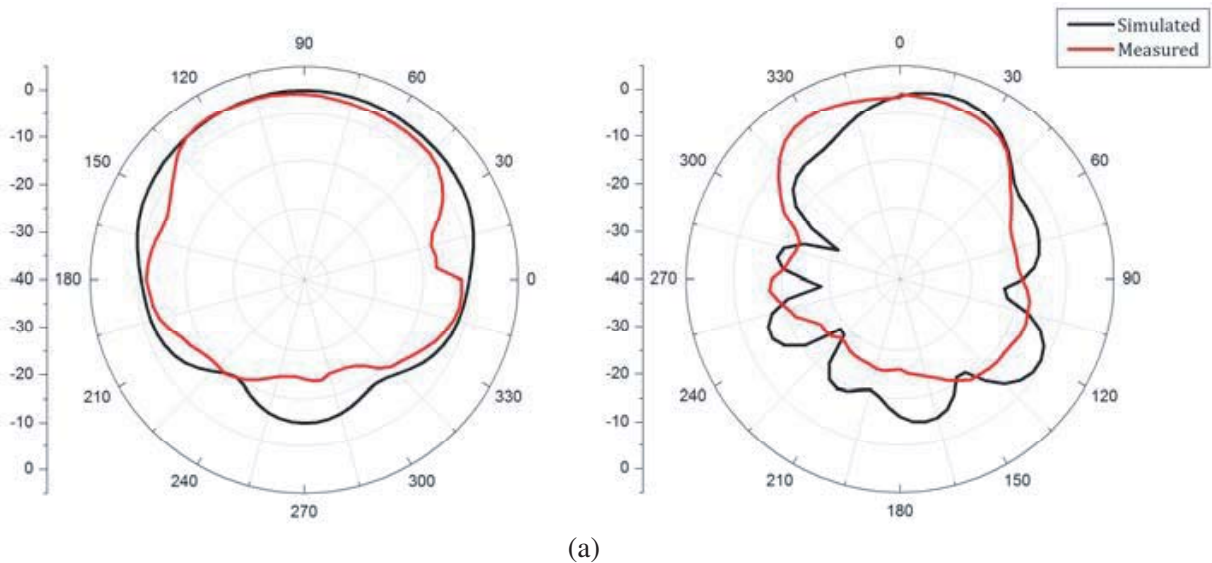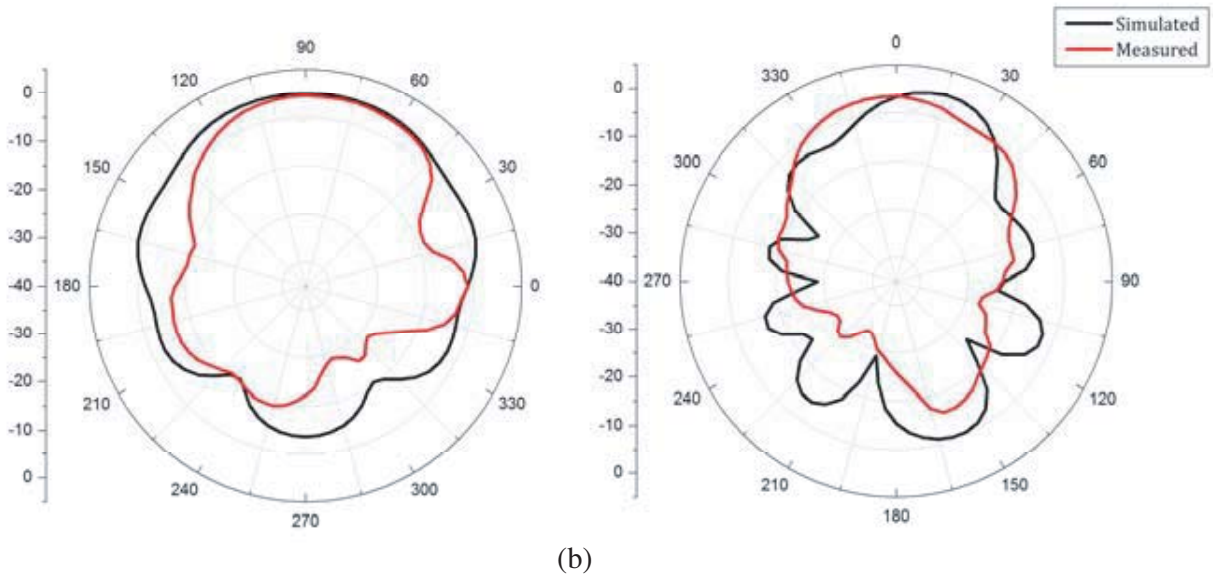
Figure 3. (a) H and E plane patterns at 25 GHz. (b) H and E plane patterns at 28 GHz.
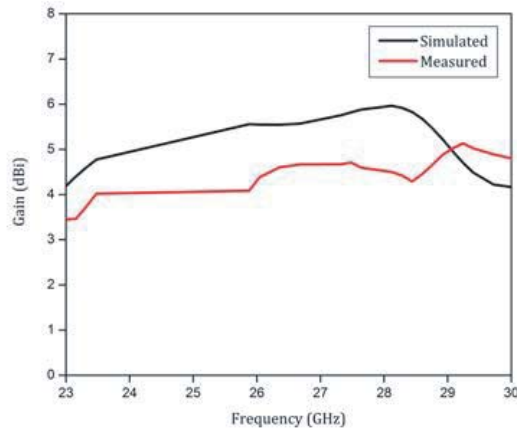
Figure 4. Endfire gain of the folded dipole.

even with a CPW feedline gap up to 350 μm. Tapered lines and quarter-wave transformers would lead to a relatively narrow band due to the frequency sensitive input impedance at the balanced CPS line of the folded dipole. A 20% wide impedance bandwidth for a mobile terminal is justified to accommodate future 5G bands near 28 GHz. The slight frequency detuning of the measured curve could be attributed to the fabrication tolerances, frequency sensitive variation of the dielectric constant and the alignment with the end-launch connector. The radiation patterns at 25 and 28 GHz are depicted in Figure 3. The patterns are stable across the bandwidth due to uniform mode excitation of the folded dipole. The beamwidth in E plane (XY plane) is 40°, and the pattern is tilted by 15° due to the radiator being offset from the phase center [16]. The narrow beamwidth is due to 1λ wide ground plane which aids in beam collimation and high front to back ratio of more than 10 dB for the 20% band. The beamwidth in the H plane (YZ Plane) is 140° and front to back ratio 10 dB.

The endfire gain varies from 4–6 dBi in the 23–30 GHz band. Gain was measured with the standard gain transfer method. The maximum deviation between simulated and measured gains is 1.6 dB as illustrated in Figure 4. Gain could be increased by 1 dB by increasing the width of the ground plane, which would also increase the physical footprint of the antenna.

3. CONFORMAL FOLDED DIPOLE

The proposed antenna is $2.1\lambda \times 2\lambda$ at 28 GHz. The occupied physical volume is relatively large given the aperture requirements for the endfire gain [16]. In order to shrink the physical size of the antenna element, additional matching circuit could be used at the expense of decreased gain. The other alternative is to conform the antenna without a significant compromise in the gain. Hence, the proposed topology of conformal antenna does not alter the radiating aperture drastically. The choice of a 20 mil substrate is justified due its flexibility to conform to the contour of the mobile terminal. Typically 5–10 mil substrates are the preferred choice but lack the structural stability for the application in question. It must also be observed that the trace width and gap would be 4.3 mm and 100 μm respectively for a 10 mil substrate leading to over-moded antenna when matched to the radiating structure. Also, the dielectric support structure for thinner substrates would lead to detuning of the antenna and create distortions in the H plane radiation patterns in addition to compromised gain. The uniplanar feed is justified for conformal structures, since conventional microstrip feed would suffer from higher discontinuity due to the bending strain on both sides of the substrate. The 17 μm copper trace on the ground plane would snap when bent creating a strong impedance mismatch due to poor transition from the feed to the radiating aperture.

(a)   (b)
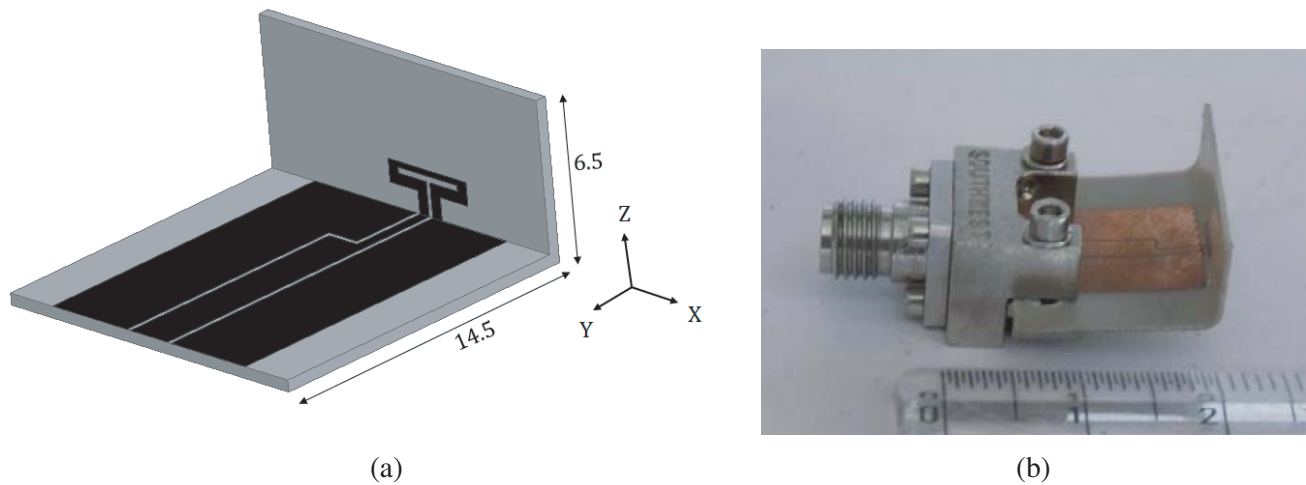
Figure 5. (a) Design of the conformal folded dipole. (b) Photograph of the conformal folded dipole.

(a)   (b)
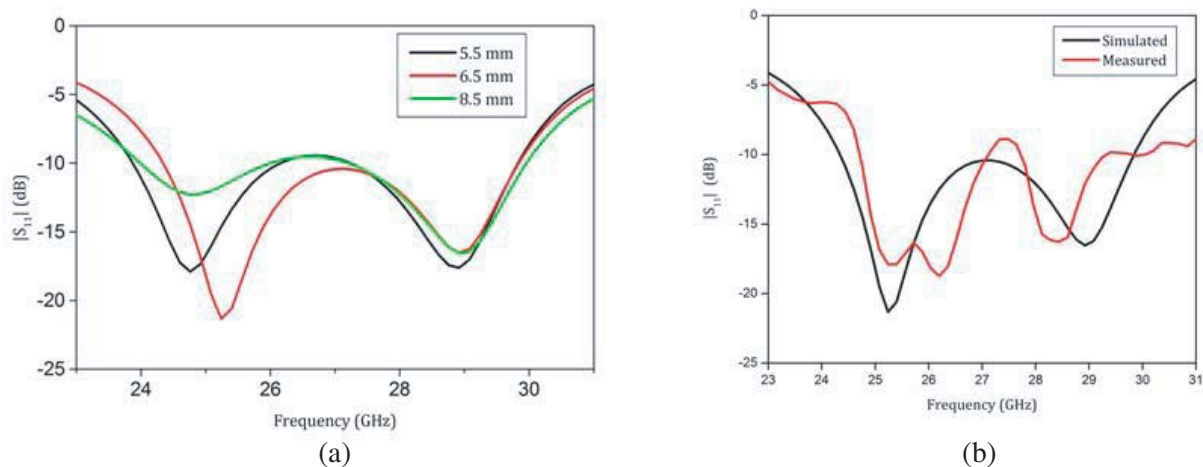
Figure 6. (a) $|S_{11}|$ variation with bending. (b) $|S_{11}|$ of the conformal folded dipole.

The topology of the conformal folded dipole is illustrated in Figure 5. The antenna is bent immediately after the stepped impedance transformer. The primary reason for a 6.5 mm bend is to create least distortion in the input impedance as evident from the bending analysis curves shown in Figure 6(a). If the antenna was conformed at the edge of the radiator, the coupling between the orthogonal ground plane and the radiator would detune the antenna element. If folded dipole is bent including the ground plane, then the back lobe would be enhanced, which could be mitigated with an electrically large aperture at least 2λ in both the dimensions which might be unsuitable for integration with mobile terminals [6]. The impedance bandwidth of the conformal antenna is from 24 to 30 GHz as depicted in Figure 6(b), it must be observed that the mismatch between planar and conformal return loss characteristics is minimal due to the reduced discontinuity in the feedline post bending. This is because of the reduced copper footprint on the top plane feeding the radiator. The deviation between simulated and measured results could be attributed to the non-ideal orthogonal bend of the fabricated structure.

H plane (YZ plane) radiation patterns are shown in Figure 7(a) at 28 and 30 GHz, and beamwidth is around 120° throughout the band. The radiation is a result of the primary folded dipole and the

(a)

(b)
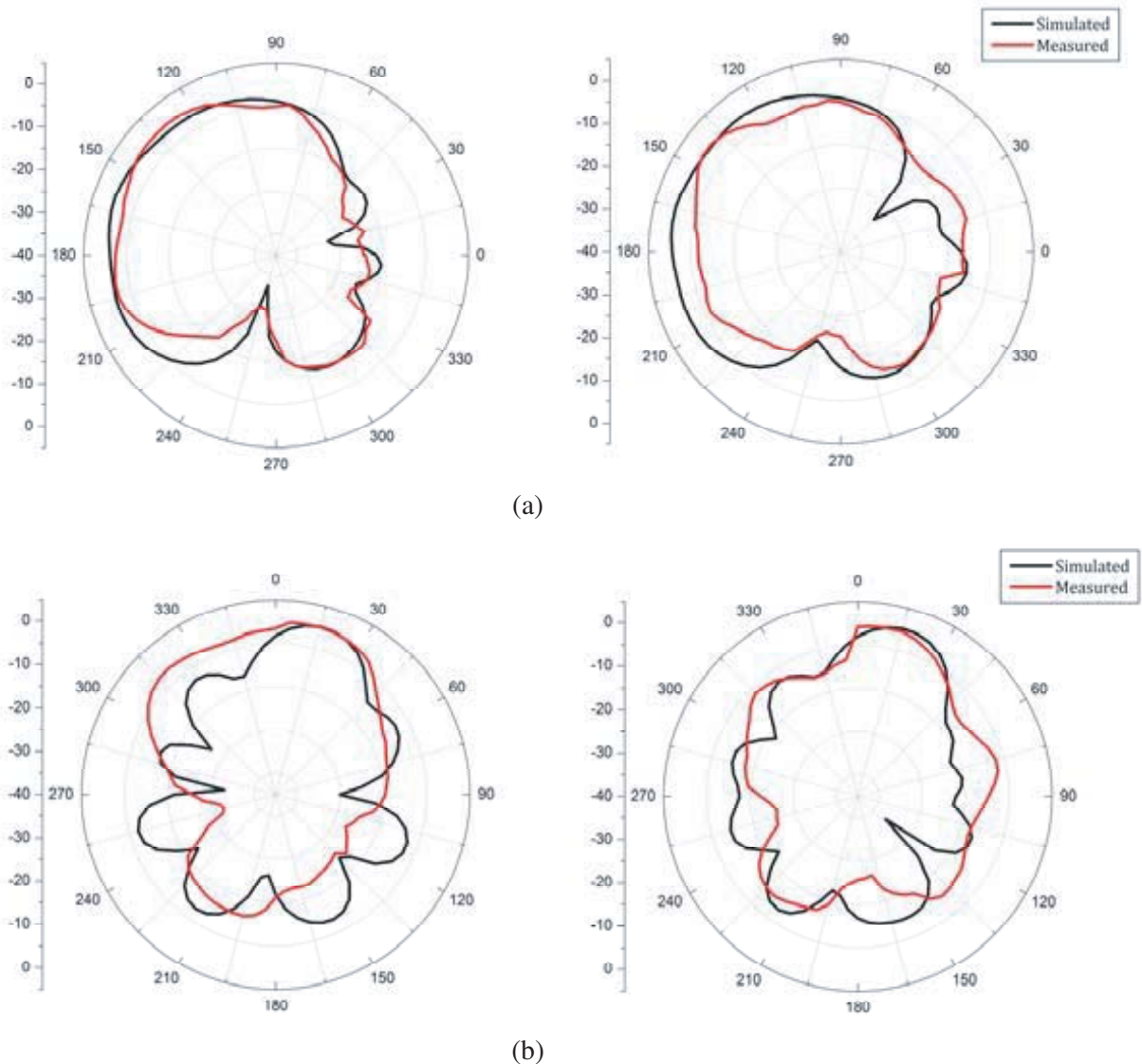
Figure 7. (a) H plane patterns at 28 and 30 GHz. (b) E plane patterns at 28 and 30 GHz.

scattering due to the orthogonal feed plane. The beam would be symmetrically distributed in the top half space when the folded dipole is elevated to around 8 mm away from the feed plane. Then the aperture of the reflector would exceed the size of the typical mobile terminal for this topology, hence 6.5 mm height is optimized for reasonable patterns in the H plane. The radiation in the range 60° to 90° indicates that the specific absorption rate would be high when integrated with the mobile terminal. E plane (XY plane) patterns at 28 and 30 GHz are illustrated in Figure 7(b), and the beamwidth is 40° with a front to back ratio of more than 10 dB across the band. This indicates that the orthogonal ground plane is still effective maintaining the pattern integrity in the E plane. The beamtilt persists even with the conformal structure due to the offset of the phase center.

The discrepancy between simulated and measured patterns is primarily due to the transitions utilized for pattern measurements in the anechoic chamber.

The endfire gain of the conformal antenna is shown in Figure 8. It varies from 1.5 to 2 dBi in the 25–30 GHz band. The low gain could be attributed to the reduced effective aperture of the conformal folded dipole antenna compared to its planar counterpart, especially the enhanced beamwidth in the H plane decreased the gain. Various gain enhancement techniques for SAR reduction could be investigated such as: localized ground plane beneath the folded dipole, and this would be operational in a narrowband with poor gain due to the available aperture for conductor backing. An absorber could be mounted behind the radiating aperture at quarter-wavelength for back lobe mitigation, and this method would reduce the impedance bandwidth and endfire gain. The third option is to strategically place a wideband reflector near the conformed aperture, which maintains the 20% bandwidth with a reasonable gain across the band.
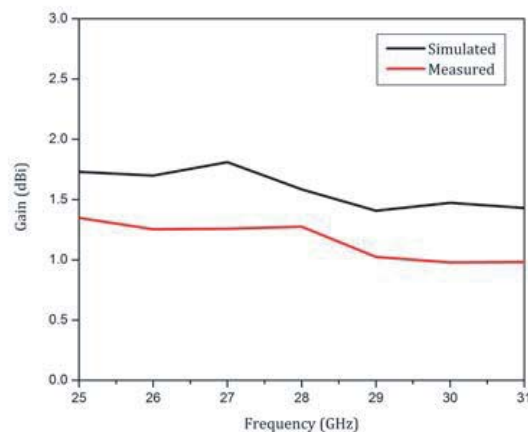
Figure 8. Endfire gain of conformal folded dipole.

4. CONFORMAL FOLDED DIPOLE BACKED BY REFLECTOR

An electrically large (at least $3\lambda \times 3\lambda$) full metallic sheet could be integrated at quarter-wavelength near the radiating aperture. But this technique decreases the impedance bandwidth of the conformal antenna, hence a wideband reflector composed of periodic structures is proposed. Also, the wideband reflector would deliver similar endfire gain and front to back ratio at a relatively smaller aperture proving its utility in integration with a typical mobile terminal. The proposed unit cell along with a photograph of the wideband reflector is shown in Figure 9. A sinusoidal slot is etched on the top plane of a Nelco NY9220 substrate with 20 mil thickness. Periodic boundary conditions were used for simulations. The length of the waveguide was optimized for dominant mode excitation, and the polarization of the incident wave was in congruence with the polarization of the folded dipole radiation. The transmission is less than 25 dB with a linear phase across the band of interest proving its utility in reflector application. It is illustrated in Figure 10.

An array of 5×5 unit cells has been designed to function as a reflector. Electrically, the reflector aperture is $0.8\lambda \times 0.8\lambda$ which is relatively compact compared to other reported designs. A 0.5 mm
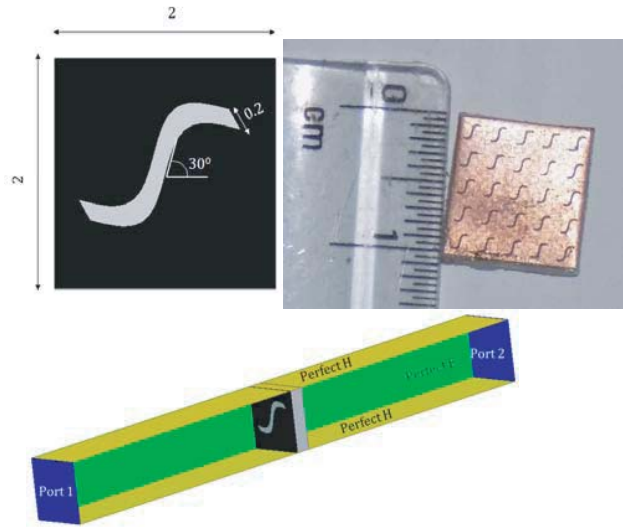
Figure 9. Unit cell of the wideband reflector.
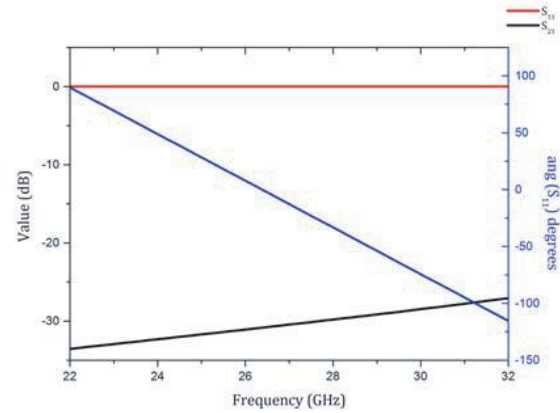
Figure 10. S_{11} and $|S_{21}|$ of the proposed unit cell.

(a)

(b)
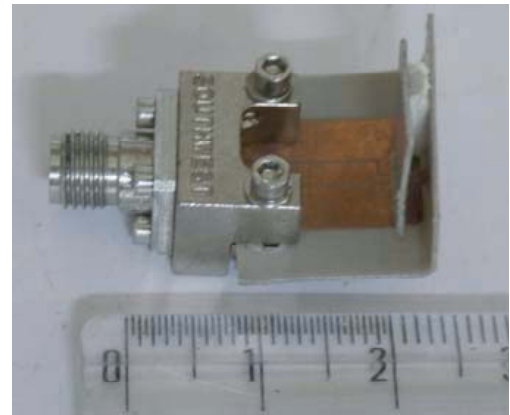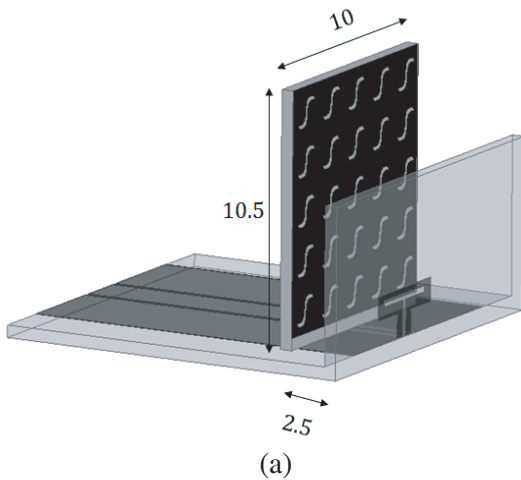
Figure 11. (a) Conformal antenna backed by reflector. (b) Photograph of the proposed antenna.

clearance is maintained between the CPW feed plane and the reflector to prevent coupling. The width of the reflector decides the beamwidth in the E plane for instance, and if a 0.5λ wide reflector is used then the beamwidth increases to $105°$ thus reducing the gain to 3.2 dBi. The height of the reflector is critical since the front to back ratio must be improved in the H plane. The schematic and photograph of the proposed antenna integrated with reflector is shown in Figure 11. It must be observed that the reflector dimensions are a compromise between effective radiating aperture and compact size for easier integration with a typical smartphone. The offset between folded dipole and the reflector is the deciding factor of impedance bandwidth and endfire gain. To create a volume efficient antenna, the reflector could be placed at 0.5 mm away from the folded dipole, but this would reduce the bandwidth, and the reflector would behave as a radiator due to most of the energy being coupled to the reflector, wherein the half-wavelength folded dipole behaves as a parasitic. If the offset is more than 3 mm, the impedance bandwidth reaches up to 25%, but the patterns get specular at the higher end of the spectrum. Hence, the offset is chosen at 2.5 mm considering the trade-off between compactness and impedance bandwidth. The input reflection coefficient of the proposed antenna integrated with reflector is depicted in Figure 12. The bandwidth is from 24 to 30 GHz, which translates to 20%. The deviation between simulated and
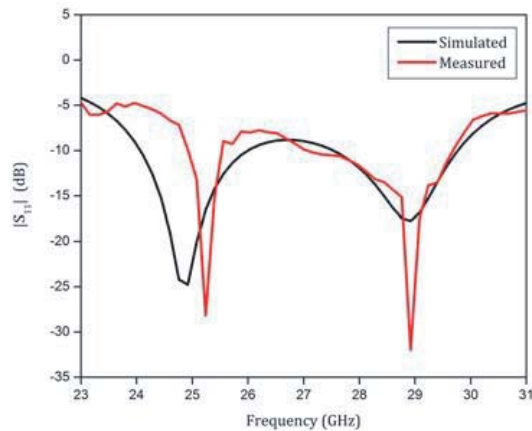
Figure 12. $|S_{11}|$ of the proposed antenna.

Figure 13. Generalized equivalent circuit of the proposed element.

measured curves is due to improper alignment between reflector and folded dipole. Also, the dielectric spacers utilized in the offset space contributes to deviation.

The generalized equivalent circuit of the conformal antenna backed by reflector is shown in Figure 13. Z_{cpw} is the characteristic impedance of the CPW feedline, which must be chosen to reduce over-moding of the antenna and to facilitate the end-launch connector fixture. The input impedance offered by the primary radiator is Z_{rad} which must be matched to the CPW feedline by a suitable impedance transformer with characteristic impedance Z_{tnr}. Z_{dis} is the stepped impedance change due to bending, which would be minimal if the transformer feed lines are electrically thin. Z_{ref} is the impedance acting in shunt by the reflector. The distance between the radiator and reflector decides the input impedance behavior. Higher impedance bandwidth could be achieved by larger gap with poor gain.

The H plane (YZ plane) patterns are illustrated in Figure 14(a) with a beamwidth of $60°$ against $120°$ without the reflector. It must be noted that with the introduction of the wideband reflector the front to back ratio has been improved to $12\,\mathrm{dB}$ across the band. The peak power is at $160°$ which translates to $+20°$ with respect to the horizontal axis of the conformal antenna. The power patterns are still suitable for integration with the 5G mobile terminals as the typical angular tilt of the mobile phone with respect to the user is around $+30°$. With an additional $20°$ tilt, the beam would be directed at $+50°$ towards the base station, which will ensure that the base station radiates at least $10\,\mathrm{dB}$ less power towards the user, and this is true for the entire 20% bandwidth. The E plane (XY Plane) patterns are shown in Figure 14(b). The beamwidth is around $70°$ with a front to back ratio of $10\,\mathrm{dB}$. The beamwidth could be further decreased with an increased reflecting aperture. It must be noted that due to the placement of the reflector the beamtilt observed in Figures 3 and 7(b) has been decreased, because of the additional offset by the reflector.

The 3D radiation patterns without and with reflector are depicted in Figure 15. It is evident that the H plane patterns have higher radiation towards the user than the E plane. Hence, the height of the reflector is critical for a reasonable reduction in SAR of the integrated mobile terminal. The beam is not uniform due to the scattering effects of the orthogonal feed plane. The proposed topology is an optimal compromise among gain, impedance bandwidth and conformity to standard mobile terminals. Gain in the peak beam is investigated with respect to the offset parameter. As observed in Figure 16,
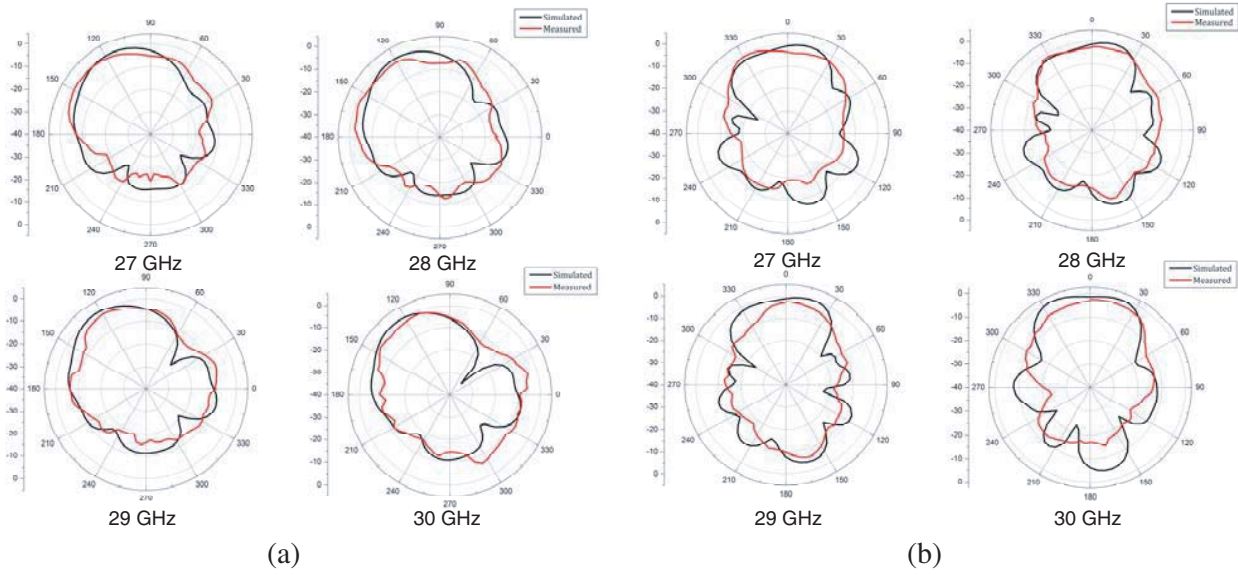
Figure 14. (a) H plane patterns from 27 to 30 GHz. (b) E plane patterns from 27 to 30 GHz.
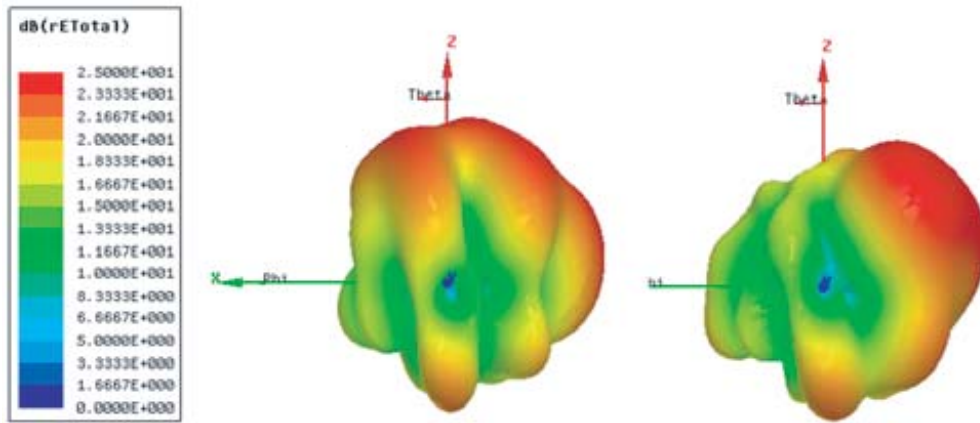
Figure 15. 3D patterns without and with reflector.

the gain has an optimum distance for maximum value. Also, increase in gain corresponds to a decrease in impedance bandwidth. The choice of the offset parameter at 2.5 mm is justified for a stable gain across the 20% bandwidth. Simulated and measured gain curves are shown in Figure 16(b). Gain varies in the range 6 to 7 dBi in the 25–31 GHz band. The discrepancy between the two curves is due to the improper mounting of the reflector with the conformal antenna. The maximum deviation is 2 dB between the two curves.

The standard adult human head model from Ansys library was utilized to study the SAR values of the proposed antenna elements. It is illustrated in Figure 17(a). A cross-section of the human head phantom was used to investigate the SAR performance of the proposed antennas, since the entire human head would be electrically larger than ($20\lambda \times 16\lambda \times 20\lambda$) which would require high performance computing for the numerical solution. The SAR values in the cross-section demonstrate the SAR behavior in the volume. The proposed conformal antennas were mounted near the ear of the head model to mimic the behavior of a typical real-world scenario. The SAR values in the cross-section of the head model without and with the reflector are illustrated in Figure 17(b). It is evident from the illustration that the reflector is effective in SAR reduction.

(a)

(b)
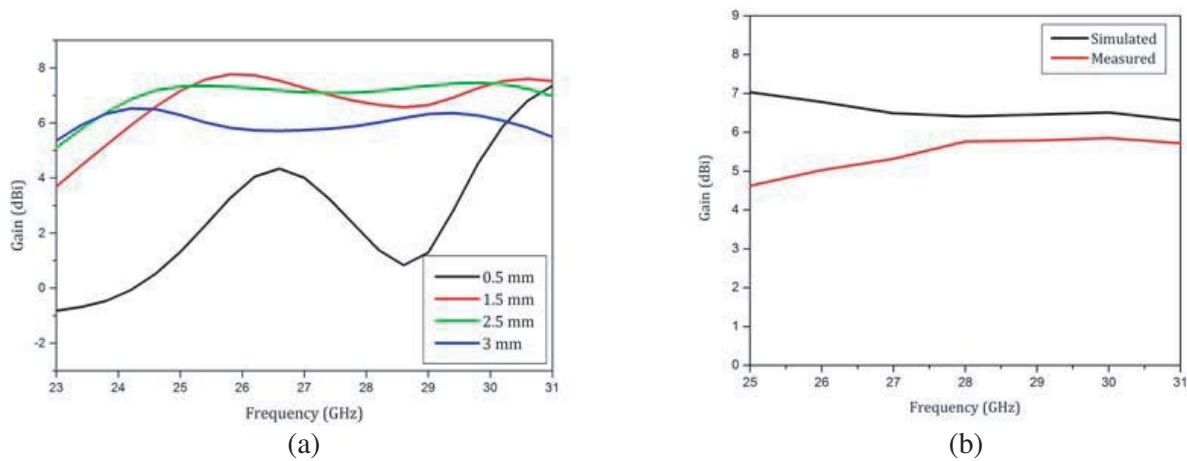
Figure 16. (a) Parametric analysis of gain with offset. (b) Gain of the proposed antenna.

(a)

(b)
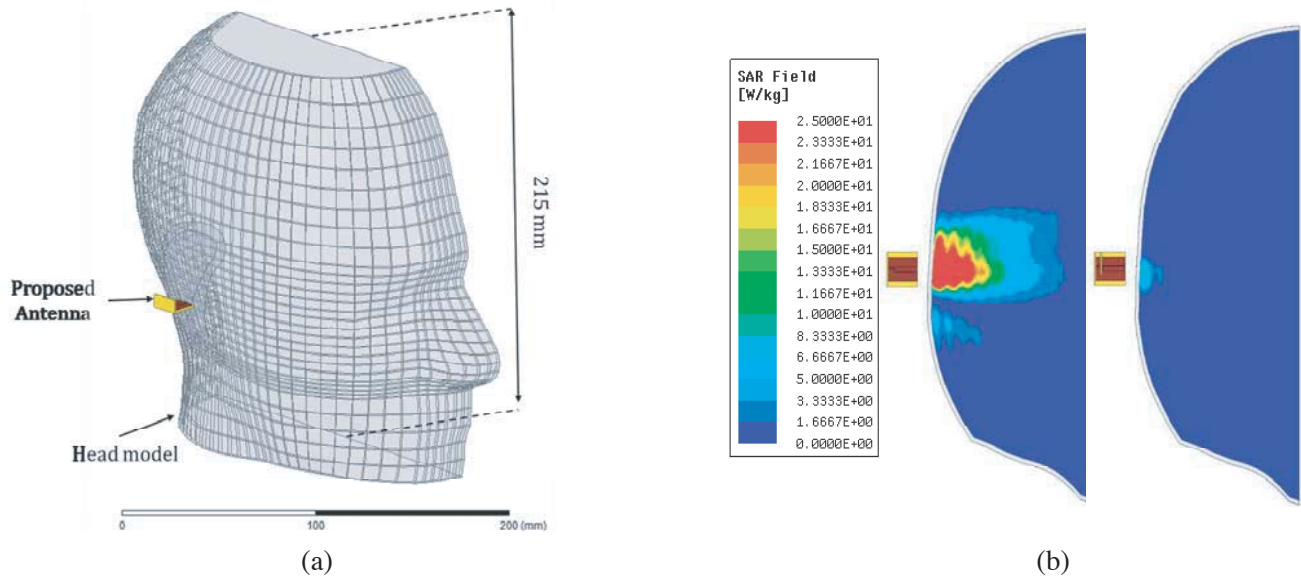
Figure 17. (a) Antenna placement with head phantom. (b) SAR without and with reflector.

The experimental measurement setup utilized for characterizing the radiation patterns of the proposed elements is shown in Figure 18. The inset of the figure shows the blown up view of the antenna under test. The standard gain Ka band antenna was used as the transmitter, and the proposed antenna mounted to the end-launch connector was used as the receiver.

Pattern diversity is also investigated for the proposed antenna, which would cater to the landscape and portrait mode in a typical phone. Two identical conformal antennas on the same substrate were modeled. The distance between the two conformal antennas was around 20 mm, and the mutual coupling was less than 30 dB. The mutual coupling increases up to 20 dB when the elements were brought close together at 10 mm. The 3D radiation patterns when the corresponding ports are excited are shown in Figure 19. The feed lengths could be reduced for further compaction. The radiation patterns are stable and almost independent of the other element, justifying the orthogonality of the radiation patterns hence proving the proposed antenna's utility in a typical mobile terminal environment.

Table 1 illustrates the design characteristics of the proposed antenna element in comparison with the reported designs in literature. It is evident that the proposed antenna has least gain variation for
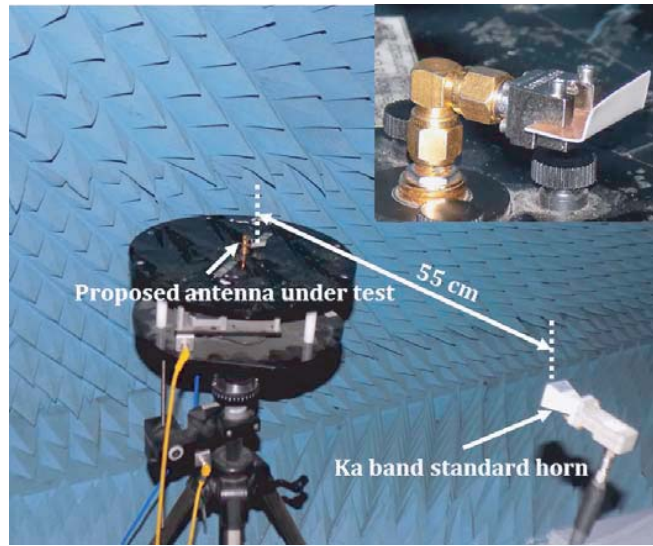
Figure 18. Measurement set-up.

(a)   (b)
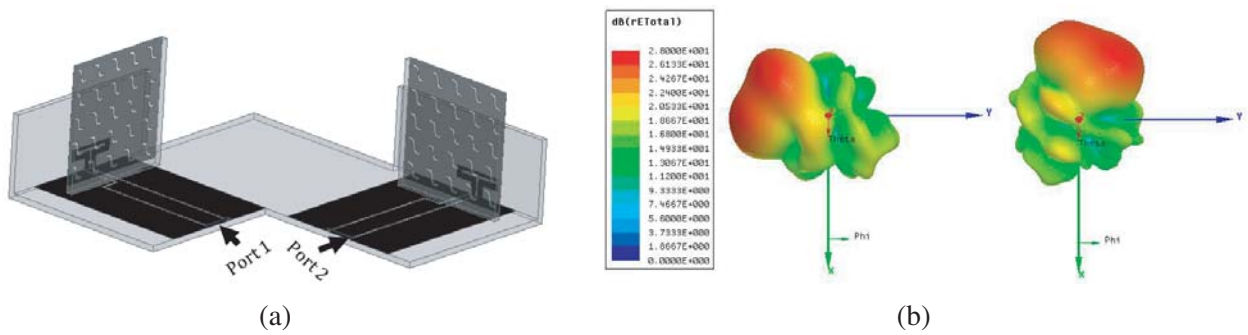
Figure 19. (a) Pattern diversity design. (b) 3D patterns when port 1 and port 2 are excited.

Table 1. Comparison with other designs.

Reference	Imp. BW (GHz)	Gain (dBi)	Feed	Conformal
[19]	24–28 (15%)	3–4.5	CPW	No
[20]	57–64 (11.6%)	8–9	Microstrip	No
[21]	22–24 (8.7%)	4–6	Microstrip	No
[22]	21–25 (17%)	8–10	CPS	No
Proposed Without reflector	24–30 (20%)	1.5–2	CPW	Yes
Proposed With reflector	24–30 (20%)	6–7	CPW	Yes

a wide bandwidth with conformal architecture, hence proving its utility as a potential candidate for future 5G mobile terminals operating in the 28 GHz band.

5. CONCLUSION

A CPW-fed folded dipole on 20 mil substrate with a 20% impedance bandwidth and an endfire gain of 4–6 dBi is presented. The conformal architecture of the element has been investigated which leads to poor front to back ratio hence increasing the SAR value when integrated with a mobile terminal. A compact $(0.8\lambda \times 0.8\lambda)$ wideband reflector is proposed and integrated with the conformal folded dipole to enhance gain and improve the patterns in the H plane resulting in a 20% wideband element with 6–7 dBi gain. Pattern diversity of the proposed element has also been explored.

REFERENCES

1. Forecast, Cisco VNI, "Cisco visual networking index: Global mobile data traffic forecast update 2009–2014," *Cisco Public Information*, February 9, 2010.
2. Wang, C.-X., et al., "Cellular architecture and key technologies for 5G wireless communication networks," *IEEE Communications Magazine*, Vol. 52, No. 2, 122–130, 2014.
3. Hong, W., K.-H. Baek, Y. Lee, Y. Kim, and S.-T. Ko, "Study and prototyping of practically large-scale mmWave antenna systems for 5G cellular devices," *IEEE Communications Magazine*, Vol. 52, No. 9, 63–69, 2014.
4. Rappaport, T. S., S. Sun, R. Mayzus, H. Zhao, Y. Azar, K. Wang, G. N. Wong, J. K. Schulz, M. Samimi, and F. Gutierrez, "Millimeter wave mobile communications for 5G cellular: It will work!," *IEEE Access*, Vol. 1, 335–349, 2013.
5. Zhang, J., X. Ge, Q. Li, M. Guizani, and Y. Zhang, "5G millimeter-wave antenna array: Design and challenges," *IEEE Wireless Communications*, Vol. 24, No. 2, 106–112, 2017.
6. Rowell, C. and E. Y. Lam, "Mobile-phone antenna design," *IEEE Antennas and Propagation Magazine*, Vol. 54, No. 4, 14–34, 2012.
7. Haraz, O. M., A. Elboushi, S. A. Alshebeili, and A.-R. Sebak, "Dense dielectric patch array antenna with improved radiation characteristics using EBG ground structure and dielectric superstrate for future 5G cellular networks," *IEEE Access*, Vol. 2, 909–913, 2014.
8. Asaadi, M. and A. Sebak, "High-gain low-profile circularly polarized slotted SIW cavity antenna for MMW applications," *IEEE Antennas and Wireless Propagation Letters*, Vol. 16, 752–755, 2017.
9. Jilani, S. F. and A. Alomainy, "Planar millimeter-wave antenna on low-cost flexible PET substrate for 5G applications," *2016 10th European Conference on Antennas and Propagation (EuCAP)*, 1–3, IEEE, 2016.
10. Park, J.-S., J.-B. Ko, H.-K. Kwon, B.-S. Kang, B. Park, and D. Kim, "A tilted combined beam antenna for 5G communications using a 28-GHz band," *IEEE Antennas and Wireless Propagation Letters*, Vol. 15, 1685–1688, 2016.
11. Sarabandi, K., J. Oh, L. Pierce, K. Shivakumar, and S. Lingaiah, "Lightweight, conformal antennas for robotic flapping flyers," *IEEE Antennas and Propagation Magazine*, Vol. 56, No. 6, 29–40, 2014.
12. Agnihotri, N., G. S. Karthikeya, K. Veeramalai, A. Prasanna, and S. S. Siddiq, "Super wideband conformal antenna array on cylindrical surface," *2016 21st International Conference on Microwave, Radar and Wireless Communications (MIKON)*, 1–4, IEEE, 2016.
13. Semkin, V., F. Ferrero, A. Bisognin, J. Ala-Laurinaho, C. Luxey, F. Devillers, and A. V. Räisänen, "Beam switching conformal antenna array for mm-wave communications," *IEEE Antennas and Wireless Propagation Letters*, Vol. 15, 28–31, 2016.
14. Si, L.-M., W. Zhu, and H.-J. Sun, "A compact, planar, and CPW-fed metamaterial-inspired dual-band antenna," *IEEE Antennas and Wireless Propagation Letters*, Vol. 12, 305–308, 2013.
15. Raman, S. and G. M. Rebeiz, "94 GHz slot-ring antennas for monopulse applications," *Antennas and Propagation Society International Symposium, 1995, AP-S, Digest*, Vol. 1, 722–725, IEEE, 1995.

16. Zhai, G., Y. Cheng, Q. Yin, S. Zhu, and J. Gao, "Uniplanar millimeter-wave log-periodic dipole array antenna fed by coplanar waveguide," *International Journal of Antennas and Propagation*, Vol. 2013, 2013.

17. Elsheakh, D. M. and M. F. Iskander, "Circularly polarized triband printed quasi-Yagi antenna for millimeter-wave applications," *International Journal of Antennas and Propagation*, Vol. 2015, 2015.

18. Jackson, R. W., "Considerations in the use of coplanar waveguide for millimeter-wave integrated circuits," *IEEE Transactions on Microwave Theory and Techniques*, Vol. 34, No. 12, 1450–1456, 1986.

19. Jilani, S. F., S. M. Abbas, K. P. Esselle, and A. Alomainy, "Millimeter-wave frequency reconfigurable T-shaped antenna for 5G networks," *2015 IEEE 11th International Conference on Wireless and Mobile Computing, Networking and Communications (WiMob)*, 100–102, IEEE, 2015.

20. Dadgarpour, A., B. Zarghooni, B. S. Virdee, and T. A. Denidni, "Single end-fire antenna for dual-beam and broad beamwidth operation at 60 GHz by artificially modifying the permittivity of the antenna substrate," *IEEE Transactions on Antennas and Propagation*, Vol. 64, No. 9, 4068–4073, 2016.

21. Alhalabi, R. A. and G. M. Rebeiz, "High-efficiency angled-dipole antennas for millimeter-wave phased array applications," *IEEE Transactions on Antennas and Propagation*, Vol. 56, No. 10, 3136–3142, 2008.

22. Alhalabi, R. A. and G. M. Rebeiz, "Differentially-fed millimeter-wave Yagi-Uda antennas with folded dipole feed," *IEEE Transactions on Antennas and Propagation*, Vol. 58, No. 3, 966–969, 2010.